Velocity Distributions of Oxygen Atoms Incident on Spacecraft Surfaces

P. N. Peters* and R. C. Sisk†
NASA Marshall Space Flight Center, Alabama
and
J. C. Gregory‡
University of Alabama, Huntsville, Alabama

The angular distributions of oxygen atoms incident on surfaces in low Earth orbit have been calculated for a number of ambient gas temperatures. Atom fluxes to surfaces were modeled by integrals over all permitted angles of incidence. Angles of incidence are limited by masking structures, and a number of types of mask were considered. Combustible surfaces exposed to the orbital atmosphere are heavily etched, creating profiles in mask shadows that are sensitive to ambient temperatures. The influence of the angular distributions on the characteristics of etched surfaces is discussed. Profiles measured for a September 1983 flight were fitted to our model profile with a temperature of 750 ± 50 K, which agrees with estimates based on solar activity at that time. Applications to sensing ambient temperatures and oxygen atom densities are discussed.

Nomenclature

dA = differential area
c = most probable speed (Maxwell-Boltzmann)
$\text{erf } X = \frac{2}{\sqrt{\pi}} \int_0^X \exp(-x^2)\, dx$
$F(X) = X^2 + \sqrt{\pi}\,[(3/2)X + X^3]\,(1 + \text{erf } X) \exp X^2$
$I(\Omega)$ = intensity of atom flux in $d\Omega$
N = oxygen atom number density
s_r = speed ratio, U/c
U = ensemble velocity (orbital velocity)
u = x component of atom velocity
V = atom velocity
v,w = y and z components, respectively, of atom velocity
$X = s_r \cos \theta_a$
x,y,z = x,y,z coordinates
θ = colatitude
θ_a = angle between U and V
θ_e = angle between U and z axis
$\sigma = s_r \cos \theta_e$
ϕ = longitude
$\chi(\sigma) = \exp(-\sigma^2) + \sqrt{\pi}\,\sigma(1 + \text{erf } \sigma)$
Ω = solid angle from dA

Introduction

THE Maxwell-Boltzmann distribution of speeds of atoms or molecules is asymmetric, but the speeds have random directions, so that the distribution is spatially symmetric as viewed from a stationary reference frame, and a Gaussian or normal distribution results from examining components parallel to any one axis. However, relative to a rapidly moving spacecraft (~ 7.8 km/s in the thermosphere between 200 and 600 km), the incidence angles of atoms striking surfaces are greatly limited. For forward-facing surfaces, the particles are incident within a narrow cone with the flux strongly peaked about normal incidence. The orbital velocity is thus a dominant factor in space-borne measurements of ambient particles. In this discussion, flux refers to the differential quantity in atoms cm^{-2}/s, while fluence refers to the flux integrated over time.

Combustible materials, such as carbon and polycarbonate plastics, exhibit heavy etching due to formation of volatile oxides from low activation energy reactions with atomic oxygen in orbit.[1-5] Studying the effects on surfaces located behind shadowing structures during exposure in orbit provides a means of investigating the thermal speed distribution of oxygen atoms in the thermosphere, as previously noted.[3]

Modeling the Angular Distribution

Surfaces on an orbiting spacecraft receive a flux of oxygen atoms that depends on the atom density, the orbital velocity, the thermal velocities of the ambient atoms, the orientation of the surfaces relative to the orbital velocity, and the presence of any objects that mask the surfaces. For a satellite in a circular low Earth orbit, the constant orbital speed combined with a Maxwell-Boltzmann distribution for the temperature of the ambient atoms represents a well-defined source that has not been satisfactorily duplicated on the ground. It may be considered as an ensemble with singular speed within which particles are in thermal equilibrium. The angular distribution of particles incident on a surface is obtained by combining the Maxwell-Boltzmann distribution with the ensemble velocity.

Nocilla[6] has considered the case of a moving ensemble of gas molecules. The angular distribution of a beam of gases scattered from a surface was determined by combining the thermal speeds of the particles with their ensemble velocity. To combine the thermal speeds with the orbital velocity, we have adapted Nocilla's method with the modification that gases passed through differential areas rather than scattered from them. An important parameter in the Nocilla model is the ratio of the translational speed of the "mass" (or ensemble) to the most probable speed. Our analogous parameter is the ratio of orbital speed to the most probable speed. We varied this parameter by adjusting the temperature.

The geometry for particles exiting a differential area dA is shown in Fig. 1 (note that the z axis is normal to the plane of the surface, and that the x,z plane is chosen so that it contains U). For surfaces pointing in the orbital direction, $\theta_e = 0$, and the atom flux is symmetrical with respect to the z axis. For a

Received Aug. 28, 1986; revision received May 3, 1987.

*Physicist, Space Science Laboratory.
†Engineer, Space Science Laboratory.
‡Associate Professor, Department of Chemistry.

Maxwell-Boltzmann distribution within the ensemble, the number $dN(u,v,w)$ of oxygen atoms with velocity components between u and $u + du$, v and $v + dv$, and w and $w + dw$ is

$$dN(u,v,w) = \frac{N}{\pi^{3/2}}\frac{1}{c^3}\exp\left\{-\frac{|V-U|^2}{c^2}\right\}dudvdw \quad (1)$$

Using the same approach as Nocilla[6] and changing to polar coordinates produces

$$dN(u,v,w) = \frac{N}{\pi^{3/2}}\frac{1}{c^3}\exp\left(-\frac{U^2+V^2-2UV\cos\theta_a}{c^2}\right)V^2dVd\Omega \quad (2)$$

Since flux is the dot product of the velocity with the area multiplied by the number density, the differential flux through dA is given by

$$d(\text{flux}) = V\cos\theta\, dN(u,v,w)dA \quad (3)$$

By integrating over all speeds from 0 to ∞ and defining and identifying a number of new terms in the equations, Nocilla[6] arrived at the expression $I(\Omega)$ for the intensity of the flux of particles in a generic solid angle $d\Omega$, which is given by

$$I(\Omega) = \frac{\exp(-s_r^2)}{\pi\chi(\sigma)}\cos\theta[1+F(X)] \quad (4)$$

The three-dimensional representation of $I(\Omega)$ is fairly difficult to illustrate, but $I(\Omega)$ for two-dimensional cross sections obtained by passing planes through the z axis at various angles ϕ and for various angles θ_e are easily plotted as illustrated in Nocilla's paper.[6] Our experimental surfaces were orbited in essentially the forward direction ($\theta_e = 0$), and we determined fluences as a function of the angle of incidence in the z,y plane, as described later, so that cross sections of $I(\Omega)$ with $\phi = \pi/2$ are appropriate. The speed ratio s_r influences the shape of $I(\Omega)$. For $s_r = 0$ (i.e., a stationary surface or zero ensemble velocity relative to the surface), $I(\Omega)$ is spherical in polar coordinates, which is the same as effusion of particles through an orifice. For an orbital speed of 7 .77 km/s and a most probable thermal speed of 1.11 km/s, $s_r = 7$, and a very elongated $I(\Omega)$ results (Fig. 2). Since representing similar fluences of particles requires similar volumes to be enclosed by $I(\Omega)$, it is impractical to draw all cross sections of $I(\Omega)$ on the same scale if s_r has a large range of values. We normalize all of our results to the same maximum, so that only relative shapes are maintained, which simplifies comparisons to etched surface profiles. The actual flux in Fig. 2 for $s_r = 7$ is many times greater in the z direction than for $s_r = 0$.

To determine how much relative etching occurs at a given point on a combustible surface, it is necessary to determine what fraction of the total fluence of atoms reaches that point. Two approaches have been considered. The first assumes an imaginary plane above the etched surface, which includes masks that shadow the surface below. This imaginary plane is divided into differential areas through which the atoms pass to the etched area; integration of all nonmasked contributions to each etch point gives the profile of atom fluence on the etched surface. The second, easier approach accomplishes the same result. By recognizing that the angular distribution of thermally spreading atoms from an imaginary area dA is the same as the angular distribution of atoms striking a similar area dA_s on the etched surface, and then identifying how masks limit the angles of incidence θ at dA_s, it is possible to integrate between the proper limits for θ and obtain the fluence at dA_s. Such determinations at each point on the etched surface provide the fluence profile, which should match the experimentally produced etch profile.

Choosing always to measure surface profiles along the y axis and aligning two-dimensional masks (e.g., slits, half-planes, etc.) along the x axis simplify the analyses since x components of velocity average to a uniform effect in the x direction. For this case, the cross section of $I(\Omega)$ for $\phi = \pi/2$ thus presents how many atoms arrive at a point on the surface as a function of angle of incidence in the z,y plane. All unshaded points receive the maximum flux (integral over all possible angles of incidence), producing a uniform etch rate. Any obstruction, or mask, above the surface limits the angles of incidence; a slit of finite width will subtend a certain angle at a point on the etched surface. This subtended angle decreases as the cosine of the viewing angle for points on a line perpendicular to the slit. Except for absolute magnitude, the etch depth at each view point is given by the area under the $I(\Omega)$ distribution between the two values of θ subtending the slit from the point. Thus, etching is maximum immediately behind the slit and decreases as $I(\Omega)$ does with θ (see Figs. 3 and 4). Making the slit narrower or elevating it higher above the surface causes the slit to subtend less angle, thus producing less etch, but the basic shape as a function of θ is similar, if $I(\Omega)$ is not changed (suitable normalizations of the etch depths give the same results). Other masking arrangements require that different limits be imposed on the integral of $I(\Omega)$. The elevated half-plane, Fig. 3, produces no shadowing beyond a θ where $I(\Omega)$ is essentially zero in one direction and produces

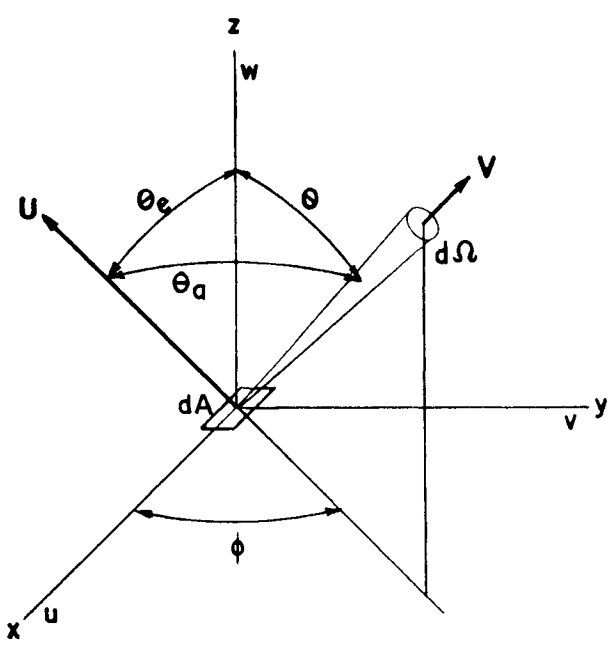

Fig. 1 Geometry for describing atoms passing through elemental area dA.

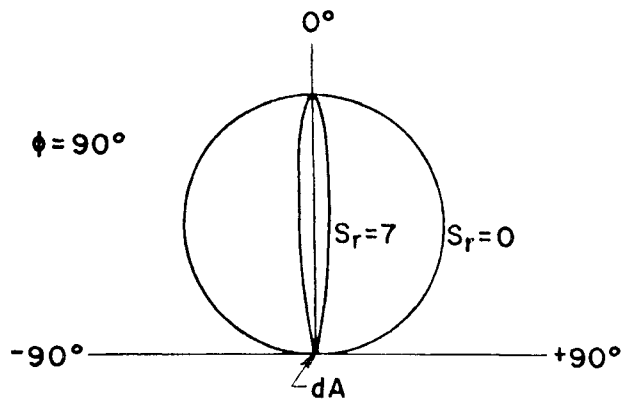

Fig. 2 Theoretical angular distributions for atom fluxes through dA for two extreme speed ratios.

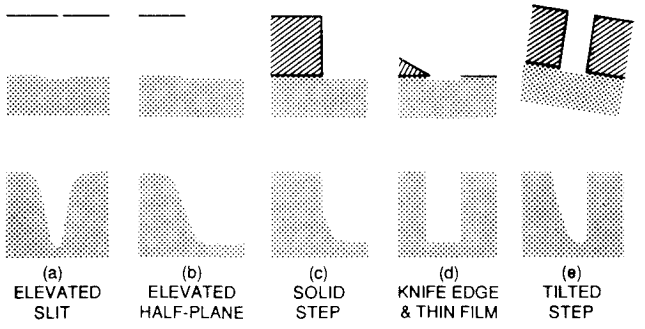

Fig. 3 Theoretical etch profiles (lower cross sections) for several masking configurations (shown schematically on top).

complete shadowing beyond the same value of θ in the opposite direction. For points between these extremes, the area under $I(\Omega)$ is partially blocked by varying amounts resulting in less flux reaching the surface at a given point. Immediately beneath the edge of the half-plane 50% of the incident particles are blocked. The flux and etch rate along the profile for the elevated half-plane is thus determined by the integral of the area under the $I(\Omega)$ distribution. This is shown as a dashed line in Fig. 4 for a temperature of 600 K; note that all curves are normalized to the same maximum, called 100%.

Similar analyses were performed for different kinds of masks. Results from such analyses and comparisons to samples flown on Shuttle flight STS-8 are discussed later. It should be noted that the relative width of $I(\Omega)$ and the etch profiles are dependent on s_r.

Experimental Technique

Since combustible solid surfaces are heavily etched by exposure to atomic oxygen in orbit, if a portion of the sensitive surface is protected by a metal mask, the shape of the edge of the etched area is affected by the angular distribution of the active oxygen atoms striking the surface. On the STS-8 flight of the Space Shuttle, a number of surfaces were exposed to the ambient oxygen in orbit as part of a materials evaluation experiment. This flight was particularly suited to the experiment discussed here because, during the entire mission, 95% of the 3.5×10^{20} atoms/cm^2 fluence was accumulated with the orbiter pointing the experiments within 1 deg of the orbital direction. A vitreous carbon disk was mounted on a heated surface that was tilted slightly (<4 deg) with respect to the velocity direction. The polished carbon surface was mounted behind a solid aluminum mask that had an effective height (thickness) of 560 μm at a hole exposing the carbon. Other combustible samples, such as CR-39 (a polycarbonate plastic), were mounted behind masks with knife edges essentially in contact with the sample surfaces, and some samples had thin film mask patterns deposited directly on their surfaces.

Surface profiles of the etched areas where mask edges existed were measured after the flight with a stylus profilometer. Theoretical etch profiles for several simple physical configurations of mask and surface were deduced for oxygen atoms striking an etchable surface partially covered by masks, as shown in Fig. 3. Comparisons of such theoretical profiles to measured etch profiles were used to estimate the average ambient temperature during exposure.

Results

Solutions to Nocilla's[6] equations are presented for temperatures of 600 and 1300 K in Fig. 4. The dashed line represents our integral from right to left of the 600-K distribution. It should be noted that, unlike Nocilla, we have normalized the maxima of all distributions to unity, so that only percentages of maximum as a function of angle are displayed. Such

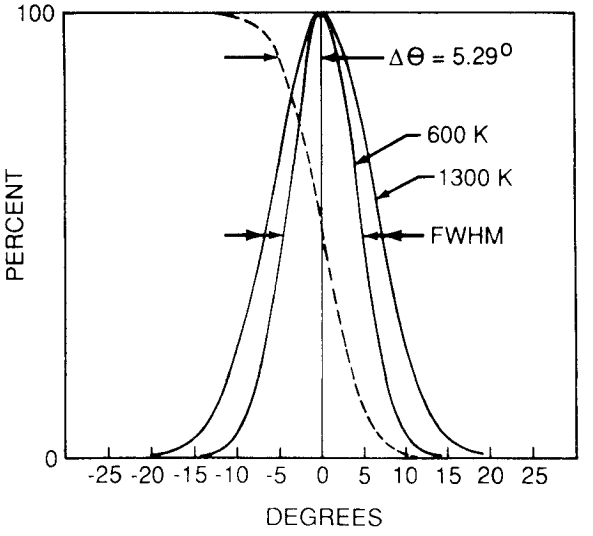

Fig. 4 Rectangular plot of the angular distributions for two temperatures. The integral of the 600-K distribution from right to left (shown dashed) relates to the etch profiles.

angular distributions can be used to visualize the "spread" that particles exhibit after passing through a small area or to describe the angles of incidence on differential areas on forward-facing surfaces.

Note, in Fig. 4, that few atoms strike forward-facing surfaces with angles of incidence exceeding 15 deg off normal. In the wake of a shielding surface with no scattering, the flux of particles at 40 deg behind the edge of a shield like Fig. 3b has been calculated for several ambient temperatures. Table 1 lists representative temperatures, speed ratios, full widths at half-maxima (FWHM) of the angular distributions, angular differences ($\Delta\theta$) between 50 and 90% fluences, and fractions of the total flux occurring at each point viewing 40 to 90 deg off the orbital direction. The FWHM and the $\Delta\theta$ angles are also defined in Fig. 4. The 50% fluence, or etch depth, level has significance in that, for a symmetrical distribution, it is the point directly below a mask edge. The 90% fluence level is simply a convenient measurement point for obtaining reasonably accurate $\Delta\theta$ that provide width comparisons of the fluence distributions or etch profiles for surfaces that receive atoms from only one side of the distribution.

A number of theoretical etch profiles have been examined as in Fig. 3. For a surface located behind a slit at a distance large compared to the slit width, the etch profile perpendicular to the slit should have the shape of an inverted angular distribution (Fig. 3a). The situation for an elevated half-plane mask is somewhat different (Fig. 3b) in that etched areas approaching the edge of the half-plane from the right receive progressively less fluence (more area under the distribution curve is blocked). Vertically under the edge, all atoms incident from the left of the edge have been blocked, reducing the maximum fluence by one-half. This reduction in fluence continues under the overhang until the effective limit for incidence angles is reached. The etch profile near a solid step mask (Fig. 3c) resembles that for the half-plane mask for the portion in front of the step but, at the step, the front face blocks additional fluence, resulting in a nearly vertical decrease in the etch depth at the step (approximately 0.1-deg maximum undercutting relative to a 560-μm mask height occurred for a 9-μm etch depth). The etch profile (Fig. 3d) that occurs near a solid knife-edge mask with edges sloped >15 deg from a normal incidence direction, or near a thin film mask deposited on the etchable surface, is nearly a vertical step.

Scanning electron micrographs, which magnify equally the horizontal and vertical dimensions, show sloped edges even

Table 1 Some characteristics of the oxygen atom fluence as a function of ambient temperature

Temp., K	Speed ratio,[a] s_r	Angular width FWHM, deg	$\Delta\theta$[b], deg	Fractional[c] flux >40 deg incidence
600	9.87	9.60	5.29	8.86×10^{-20}
700	9.13	10.36	5.70	2.78×10^{-17}
800	8.54	11.06	6.06	2.12×10^{-15}
900	8.06	11.70	6.44	6.06×10^{-14}
1000	7.64	12.32	6.77	9.21×10^{-13}
1100	7.29	12.90	7.07	8.22×10^{-12}
1200	6.98	13.44	7.39	5.26×10^{-11}
1300	6.70	13.97	7.69	2.64×10^{-10}
1400	6.46	14.48	7.95	1.00×10^{-9}
1600	6.04	15.44	8.49	9.11×10^{-9}
1800	5.70	16.32	8.97	5.09×10^{-7}
2000	5.40	17.16	9.45	2.03×10^{-7}

[a]Based on an orbital speed of 7.77 km/s, divided by the most probable speed for the Maxwell-Boltzmann distribution at given temperature.
[b]Angular difference between 50 and 90% fluences on one side of the distribution.
[c]Fraction of the total incidence flux that would be received at a point 40 deg behind the edge of the shield configuration in Fig. 3b.

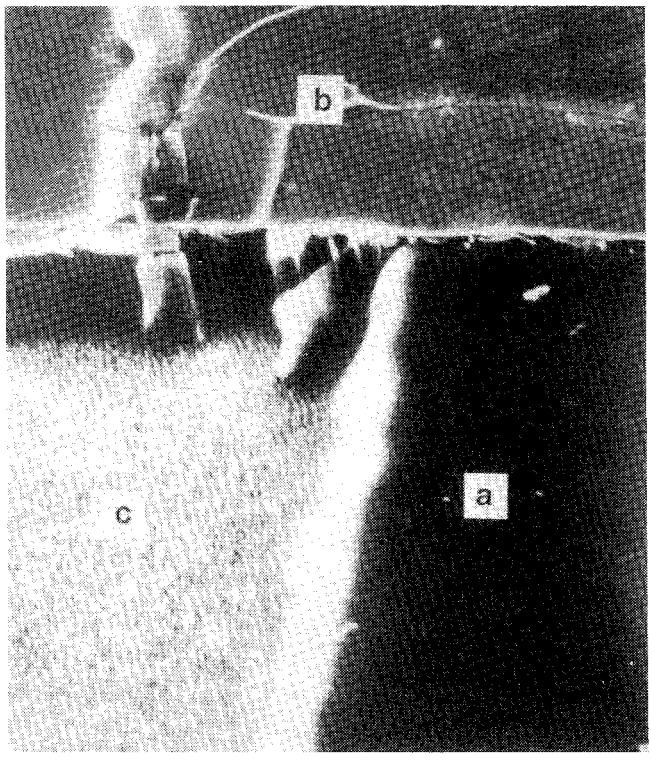

Fig. 5 Scanning electron micrograph of an etched CR-39 plastic surface.

for the etched steps near thin film masks (Fig. 5). The slopes result from microscopic shadowing by slightly elevated knife edges or by the etch steps themselves (self-shadowing). The height of the etch steps continuously increase with etch depth. The slopes of any etched edges should extend less than 15 deg relative to the top edge of the shadowing structure for normally incident atoms; thus, the extent of the shadow increases with mask height. A particle, or other contaminant, on the surface would initially mask an area its size, but as etching progresses, the shadowed area expands, with most of the fluence shadowing occurring within 7 deg of the orbital velocity direction and limited essentially to less than 15 deg. This general profile and limit appears consistent with scanning electron micrographs of etched surfaces (Fig. 5). One diffuse etch step (oriented vertically in Fig. 5) occurred near a slightly elevated knife edge of an aluminum cover (originally over area a), while another sharp etch step (oriented horizontally in the same figure) occurred at the edge of a niobium thin film pattern deposited over area b on the surface prior to etching. Both steps are similar to the profiles in Fig. 3 except that the heights of the shadowing structures were small and increased by relatively large amounts with etch depth. Fine microstructures (spiked region in area c of Fig. 5) are observed on most etched structures (even amorphous plastics) and are undoubtedly influenced by this self-shadowing effect. It is postulated that contaminants, or fine particles on the surface, provided masking and that self-shadowing created the sloped sides. Accommodation of the fast oxygen atoms may have a lower efficiency at glancing incidence to the surface, but further studies are needed to test these hypotheses. Similar spiked structures have been observed on ground-based ion-bombarded surfaces.[7] Precleaning has eliminated such structures in semiconductor device fabrications.[8] Thermal velocities within ground-based plasmas, combined with ensemble velocities created by electrical accelerations used in sputtering, should create shadowing effects similar to those in orbit, as suggested by the etched structures described above; however, the ensemble velocities of 100–2000-eV sputtering particles are higher than orbital velocities, and correspondingly higher thermal velocities would be needed to obtain much spreading within the mask shadows. Simple plasma discharges without well-defined accelerating potentials might provide a range of s_r speed ratios, depending on experimental conditions, thus varying the topography of the etched surfaces. Studying such topographies could enable researchers to gain additional knowledge about conditions within the plasmas (e.g., values of s_r) that could be compared to flight conditions. Similarly, ground-based beams can be studied and compared to other sources by examining etched surfaces.

Actual stylus tracings of some samples flown on STS-8 are shown in Fig. 6. Note that stylus traces greatly magnify the vertical dimensions compared to the horizontal. One tracing (Fig. 6a), which was taken from a vitreous carbon surface that was at the base of a 560-μm-thick solid step, is typical for near alignment of the step with the orbital direction (within 1/2 deg). Corrections for a chipped edge, an error due to the stylus shank contacting the etch step, and contaminant-created peaks are shown by a dashed line (Fig. 6a). Other examples of etched vitreous carbon surfaces where the mask step faces were not aligned with the orbital direction are shown (Figs. 6c and 6d), and the excellent steps obtained with niobium thin film masks (Fig. 6b) demonstrate the advantages of this type of mask for determining etch rates and reaction efficiencies, especially for rapidly etched materials such as the polycarbonate (CR-39) shown in Fig. 6b, where nearly 22-μm etch depth occurred for a fluence of 3.5×10^{20} atoms/cm^2.

The measured etch profile was digitized and compared to computed fluence profiles. Etching was assumed proportional to fluence, and results were obtained for different ambient gas temperatures. Comparisons were obtained by normalizing the maximum fluence to the maximum etch depth observed and requiring half-etch depths to align laterally at zero angle of incidence (Fig. 7). This procedure indicated that the average temperature of the oxygen atoms was 750 ± 50 K for the best fit, obtained by visual comparisons of two data profiles with theoretical profiles for various temperatures. All measured points fell between 700 and 800 K profiles, providing a conservative estimate of the precision. Measured and theoretical profiles were further compared by examining their angular differences between 50 and 90% maximum etch depths. Figure 8 shows the theoretical relationship between temperature and this angular difference in degrees, which is satisfied to within 1% by $T = 24.70\,(\Delta\theta)^2 - 27.37\,(\Delta\theta) + 54.60$, as obtained by a quadratic fit. An estimation of $\Delta\theta = 5.9$ deg ± 0.1 deg between the 50 and 90% etch levels shown in Fig. 7 provides the result $T = 753 \pm 26$ K.

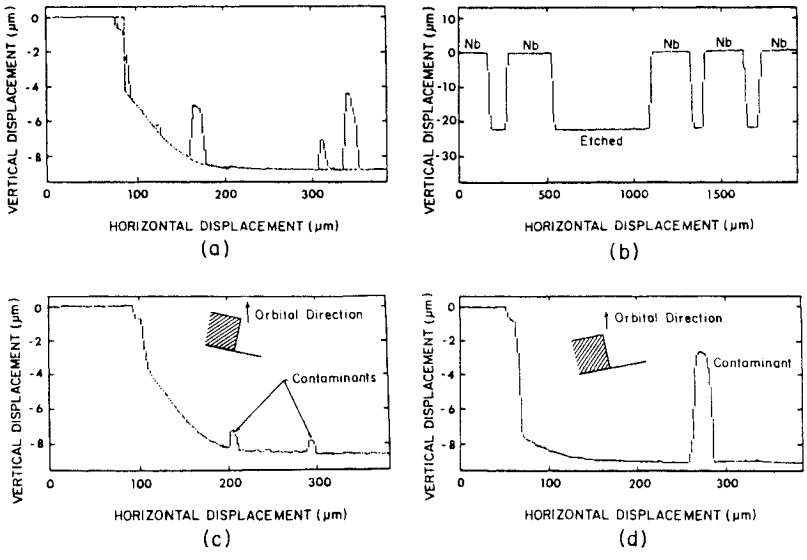

Fig. 6 Stylus profilometry tracings taken from samples flown on STS-8.

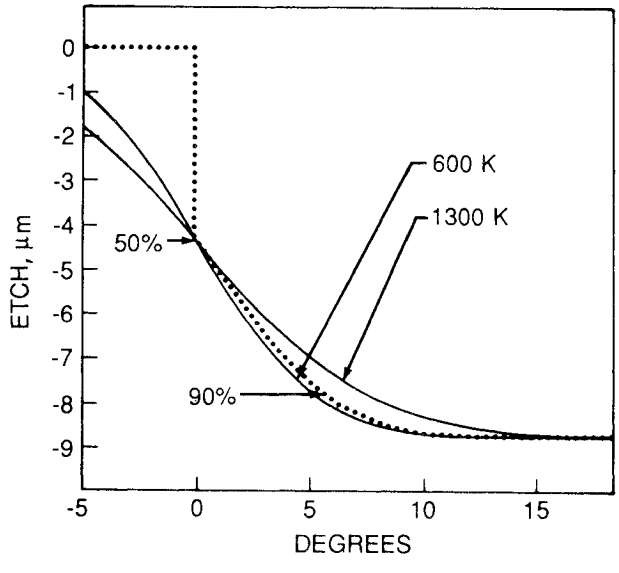

Fig. 7 Comparison of a measured etch profile with the theoretical profiles for 600- and 1300-K ambient temperature.

Discussion

Although atomic oxygen bombardment might be used beneficially for cleaning some surfaces contaminated with hydrocarbons or other combustible materials, the observed spiked erosion can seriously degrade mechanical and optical surface properties if gross etching is involved.[5] The erosion may also be used as a quantitative sensor of atomic oxygen, provided that mechanisms of processes described in this paper are understood.[9] The usual treatments of equilibrium thermodynamic variables, such as pressure and temperature, have to be modified for observations in orbit, since the orbital velocity greatly exceeds thermal velocities and incident particle velocities are highly directional. Except for outgassed or accommodated species traveling with the satellite, the orbital velocity dominates relative collision velocities between neutral thermospheric species and the orbiting surfaces.

Atoms reflected from the front faces of mask steps could be a source of additional etching, but small cross sections (for steps oriented as in Fig. 3c) and broad scattering (due to accommodation) appear to reduce this effect below the accuracy of the profile measurements discussed here; however, higher sensitivity reflection measurements of a different nature have been reported for a surface oriented at 55 deg with the velocity vector.[10]

Aligning all etch profiles so that they cross at the 50% etch depth was justified on the basis that, for symmetrical angular distributions, half of the total fluence is received for angles of incidence on each side of normal incidence; thus, the profiles all pass through 50% etch depth at 0 deg. Asymmetrical distributions (nonequilibrium thermally) and large off-normal alignments of surfaces with the orbital velocity direction could require corrections. If the vertical portion of an etch profile associated with a solid step does not occur at the 50% etch depth, the top edge of the step tilts relative to its base (exaggerated in Figs. 6c and 6d). For small tilts, the angle can be approximated by arctangent of horizontal separation between vertical slope and 50% etch divided by the mask height; e.g., arctangent (12.8/560) = 1.3 deg is an estimate for Fig. 6c. An estimate of 4.5 deg for Fig. 6d seems slightly high and may indicate that a correction is needed. The masking step for Fig. 7 was aligned to better than 0.5 deg.

The theoretical and measured etch profiles matched extremely well, considering that the etched surface received a total fluence that was integrated over 41.2 h with contributions from various latitudes and during day and night conditions. During the STS-8 mission, ambient temperatures varied from approximately 690 to 1000 K, based on extreme conditions and application of mass spectroscopy incoherent scatter (MSIS) and MSFC/J70 thermospheric models. An estimated average of 826 ± 165 K resulted from the latter model.

In the absence of scattering from surfaces, charged particle influences, outgassing, etc., integrals over appropriate ranges of the angular distribution curves provide values for oxygen atom fluences in the ultrahigh vacuum regions behind structures such as wake shields. Table 1 shows percentages of total fluence received at an arbitrary point 40 deg behind the edge of a shield like Fig. 3b. Corresponding static pressures that would produce similar fluence levels are very small since average total fluences at a typical temperature of 1000 K and an altitude of 300 km would be $\sim 10^{15}$ cm^{-2}/s, which is similar to fluences to surfaces in a static pressure of 10^{-6} torr. Thus, at 1000 K, the fluence at 40 deg behind a half-plane shield would be $\sim 10^{-12} \times 10^{15}$ cm^{-2}/s or 10^{3} cm^{-2}/s. A similar fluence would be produced by a pressure of $\sim 10^{-18}$ torr. Although the fluence behind shields is obviously strongly dependent on temperature (Table 1), it is unlikely that equilibrium thermal distributions of ambient particles at orbital altitudes contribute significantly to fluences at positions greater than 40 deg behind the edges of shields (increasing the atom density an order of magnitude above average and applying data for 2000 K gives $\sim 10^{9}$ cm^{-2}/s, which is comparable to 10^{-12} torr).

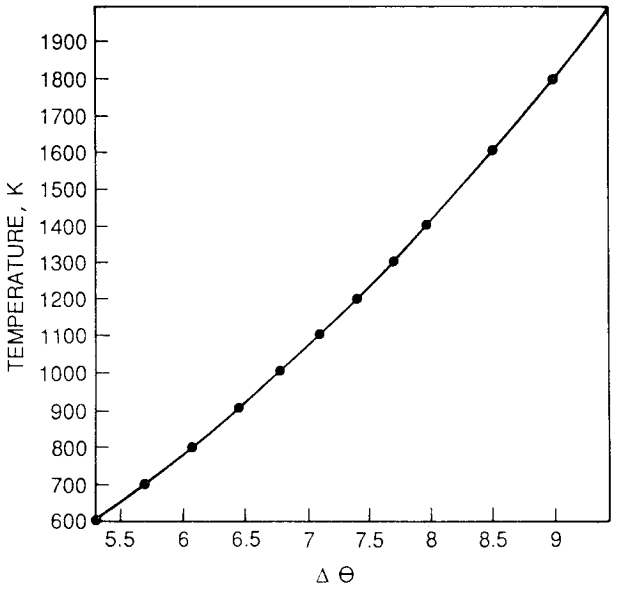

Fig. 8 Theoretical temperature angular difference ($\Delta\theta$) between 50 and 90% etch depths, or fluences, for a surface masked as in Fig. 1c.

Summary

Theoretical angular distribution profiles for oxygen atoms incident on surfaces or exiting behind masks have been calculated in an orbiting reference frame. These profiles are dependent on the ratio of the orbital speed to the most probable thermal speed of the ambient oxygen atoms. The profiles of etched combustible surfaces have been measured and related to such distribution profiles. A temperature of 750 ± 50 K, consistent with the mean ambient temperature at this altitude and for the solar activity during exposure, was obtained. Calculated profiles for a number of mask/substrate configurations were given. Microstructural and other details of etched surfaces were discussed.

Acknowledgments

We wish to thank Ms. Alice Dorries for the scanning electron photomicroscopy. We are grateful to the University of Alabama in Huntsville Research Institute for a grant for the hardware fabrication and to Dr. Lubert Leger and Mr. James Visentine for their support concerning flight requirements and data. Very helpful discussions and estimates of the thermospheric temperatures during orbit were provided by Dr. Marsha Torr and Mr. Dale Johnson. Work at UAH was supported in part by NASA Grant NAGW-823 and NASA Contract NAS8-36645.

References

[1]Gregory, J.C. and Peters, P.N., "Interaction of Atomic Oxygen with Solid Surfaces at Orbital Altitudes," *Proceedings of the First LDEF Mission Working Group Meeting,* NASA Langley Research Center, 1981, p. 48.

[2]Leger, L.J., "Oxygen Atomic Reaction with Shuttle Materials at Orbital Altitudes," NASA TM-58246, May 1982.

[3]Peters, P.N., Linton, R.C., and Miller, E.R., "Results of Apparent Atomic Oxygen Reactions on Ag, C, and Os Exposed during the Shuttle STS-4 Orbits," *Geophysical Research Letters,* Vol. 10, July 1983, pp. 569–571.

[4]Fraundorf, D. et al., "Erosion of Mylar and Protection by Thin Metal Films," AIAA Paper 838, Oct. 1983, pp. 131–137.

[5]Peters, P.N., Gregory, J.C., and Swann, J.T., "Effects on Optical Systems from Interactions with Oxygen Atoms in Low Earth Orbits," *Applied Optics,* Vol. 25, April 1986, pp. 1290–1298.

[6]Nocilla, S., "The Surface Re-emission Law in Free Molecule Flow," *Rarified Gas Dynamics,* edited by J.A. Laurmann, Academic Press, New York, 1963, pp. 327–346.

[7]Auciello, O. and Kelly, R. (eds.), *Ion Bombardment Modification of Surfaces,* Elsevier, New York, 1984, p. 466.

[8]Wang, D. and Wong, J., "Etched Trenches Conserve Semiconductor Device Space," *Research & Development,* Vol. 27, Jan. 1985, pp. 107–112.

[9]Gregory, J.C. and Peters, P.N., "The Production of Glow Precursors by Oxidative Erosion of Spacecraft Surfaces," NASA CP-2391, edited by J.H. Waite Jr. and T.W. Moorehead, May 1985, pp. 144–179.

[10]Gregory, J.C. and Peters, P.N., "A Measurement of the Angular Distribution of 5 eV Atomic Oxygen Scattered off a Solid Surface in Earth Orbit," *Proceedings of the 15th International Symposium on Rarefied Gas Dynamics,* Vol. I, edited by V. Boffi and C. Cercignani, Teubner, Stuttgart, Germany, 1986, pp. 644–656.